Biophysical Chemistry 20 (1984) 333–345
Elsevier

BPC 00888

FLUORESCENCE DECAY OF 1-METHYLPYRENE IN SMALL UNILAMELLAR L-α-DIMYRISTOYLPHOSPHATIDYLCHOLINE VESICLES.

A TEMPERATURE AND CONCENTRATION DEPENDENCE STUDY

M. VAN DEN ZEGEL, N. BOENS * and F.C. DE SCHRYVER
Department of Chemistry, K.U. Leuven, Celestijnenlaan 200F, B 3030 Leuven, Belgium

Received 7th February 1984
Revised manuscript received 18th June 1984
Accepted 22nd June 1984

Key words: Fluorescence decay; 1-Methylpyrene; Small unilamellar vesicle; L-α-Dimyristoylphosphatidylcholine

The fluorescence decay kinetics of 1-methylpyrene in small unilamellar L-α-dimyristoylphosphatidylcholine vesicles above the phase transition temperature has been studied as a function of concentration and temperature. When the 1-methylpyrene/phospholipid ratio equals 1 : 2000 no excimer is observed and the fluorescence decay is monoexponential. When this ratio is equal to or higher than 1 200, excimer is observed and the monomer and excimer decays can be adequately described by two exponential terms. The deviation of the monomer decays from monoexponentiality cannot be described by a model where the diffusion-controlled excimer formation is time dependent. The observed decays are compatible with the excimer formation scheme which is valid in an isotropic medium. The activation energy of excimer formation is found to be 29.9 ± 1.4 kJ/mol. The (apparent) excimer formation constant and the excimer lifetime at different temperatures have been determined. The diffusion coefficient associated with the excimer formation process varies between 2×10^{-10} m^2/s at 70 °C to 4×10^{-11} m^2/s at 25 °C.

1. Introduction

Vesicles are frequently used models for natural membranes. Lateral diffusion of molecules in the bilayer can be studied with fluorescence using excimer formation. The coefficient of lateral diffusion, D, of aromatic molecules in the hydrophobic region of multilamellar vesicles was studied with excimer formation using the intensity ratios of the excimer and monomer fluorescence and the 'single excimer lifetime' [1]. The method is based on the fact that excimer formation of most molecules is diffusion controlled in an isotropic medium [2,3]. At the same time, experiments performed by Vanderkooi and Callis [4] showed, using nonstationary fluorescence methods, that the classic kinetic scheme of excimer formation is not valid in lipid vesicles. They explained the nonexponential decay of the pyrene monomer fluorescence by a model which is based on the general time-dependent diffusion theory of Smoluchowski [5]. In a following paper, Vanderkooi and co-workers [6] found a better fit to their experimental data of pyrene fluorescence in dimyristoylphosphatidylcholine vesicles when a two-dimensional diffusion theory was used. They obtained a diffusion coefficient of 3×10^{-12} m^2/s for pyrene in dimyristoylphosphatidylcholine vesicles at 30 °C. No temperature study was done by these authors.

A few years later Liu et al. [7] studied the fluorescence decay kinetics of pyrene in vesicles above and under the phase transition temperature. They found experimentally that the decay of the monomer fluorescence of pyrene in di-

---

* To whom correspondence should be addressed.

palmitoylphosphatidylcholine vesicles could be fitted to a three-exponential decay law and that it could not be explained by the time-dependent diffusion theory as suggested by Vanderkooi and Callis [4]. Liu and co-workers did not perform a concentration dependence study and their samples were not degassed. They suggested an alternative kinetic scheme involving excited-state interaction, but they did not prove that their scheme was valid.

Our present work is a concentration and temperature dependence fluorescence decay study of excimer formation of 1-methylpyrene above the phase transition temperature in L-α-dimyristoyl phosphatidyl choline (DMPC) vesicles. We worked with small unilamellar vesicles (SUV) because these are well defined membrane systems [8], stable above the phase transition temperature [9] and better suited for a fluorescence study than the larger systems like multilamellar vesicles because they scatter less in the wavelength region where the probe is excited.

2. Materials and methods

2.1. Chemicals

DMPC was obtained from Sigma Chemical Co. Thin layer chromatography (solvent, chloroform: methanol: water 65 : 25 : 4: I_2 staining) showed a single spot. 1-Methylpyrene was prepared by the method of Huang-Minlon [10] and was recrystallized from ethanol with carbon black, followed by column chromatography on silica gel with hexane as eluent. Its purity was checked by fluorescence lifetime measurement in isooctane (255 ns). KCl (Aldrich Gold Label) was used without any further purification. SDS (Merck, for biochemical research) was purified by repeated recrystallization from methanol. The purity was checked by measurement of the critical micelle concentration (0.00794 M, 25 °C). Chloroform (Fluka reagent grade), isooctane (Aldrich Gold Label) and bidistilled-deionized water were used as solvents.

2.2. Membrane preparations

SUV were prepared from DMPC [8,11–13]. 70 mg of the phospholipid were dissolved in chloroform. An appropriate amount of probe was added from a stock solution and the chloroform solution was lyophilized for 12 h in the dark. 12 ml of a 50 mM KCl solution were added. The solution was saturated with pure argon and sonicated with a Heat Systems sonifier (W 375) with the output control at 7 and pulsed with 70% 'duty cycle'. Sonication was carried out intermittently for 3 min, followed by a 1 min rest period for a maximum sonication time of 45 min. Following sonication, the dispersion was centrifuged for 30 min at 100 000 × *g*. A Beckman L 65 centrifuge with an SW 50.1 fixed angle rotor was used. The supernatant was removed and was further centrifuged for an additional 60 min at 100 000 × *g*. 4 ml of the top material were pipetted into a 1 cm^2 quartz fluorescence cell and flushed with argon for 15 min. The cell was then closed with a two-way valve. During the whole preparation the phospholipid sample was kept above the phase transition temperature.

2.3. Determination of concentrations

Phospholipid concentrations were determined using the method of Petitou et al. [14]. The phospholipid concentration was 5.45 ± 0.1 mM in all the different preparations. The probe concentration was determined using steady-state fluorescence intensities. A small amount of the samples was diluted in an appropriate amount of a 10^{-2} M SDS solution. This solution was degassed by the freeze-pump-thaw method on a high vacuum line ($< 10^{-4}$ Torr). The fluorescence intensities were measured with a Spex Fluorolog and the probe concentrations were determined using a standard curve of 1-methylpyrene (10^{-6}–10^{-5} M) in equimolar SDS solutions. The probe/phospholipid ratios experimentally determined agreed within 5% error with the probe/phospholipid ratios in the initial chloroform solution.

2.4. Fluorescence decay experiments

The fluorescence decay curves of the samples were obtained using the time-correlated single-photon counting technique [15,16]. All samples were measured within 15 h after vesicle preparation and were always kept above the phase transition temperature. The samples were contained in home-built 1-cm^2 quartz fluorescence cuvettes. The samples were deoxygenated by flushing with argon for 15 min before measurement. The cuvettes were closed with a two-way Teflon valve. The temperature of the samples was kept constant by circulating water through the cell holder. The temperature stability was better than 0.1 K. A diagram of the subnanosecond time-resolved fluorometer used for the fluorescence decay measurements reported in this paper is shown in fig. 1. Sample excitation in the wavelength range 290–315 nm was achieved with a frequency-doubled, cavity-dumped, mode-locked synchronously pumped dye laser system. An extended cavity 5 W argon ion laser (Spectra-Physics model 16509) was mode-locked using an ultra-stable mode-locking system (Spectra-Physics model 342A) giving pulses of about 150 ps (full width at half-maximum intensity), at a repetition rate of 82 MHz, and with an average power of 300 mW. These pulses were used to excite rhodamine 6G dye in ethylene glycol (purchased from Spectra-Physics) in a jet stream dye laser (Spectra-Physics model 375B) with a cavity length equal to that of the ion laser. An acousto-optic cavity dumper (Spectra-Physics model 344S) and cavity dumper driver (Spectra-Physics model 454) were used to emit pulses at a rate of 400 or 800 kHz. Wavelength tuning was performed with a tuning wedge (Spectra-Physics model 375) incorporated in the dye laser cavity. After careful alignment average powers of 18 mW could be obtained at a pulse repetition rate of 800 kHz. The pulse width was approx. 10 ps as measured with an Applied Photophysics autocorrelator. Frequency doubling was achieved with an angle-tuned Inrad model 563-1117 KDP 'B' crystal. The residual undoubled light was removed with a Corning 7-54 filter. The laser system was mounted on a mechanically isolated optical table (Newport Research Corp.) in a temperature- (20 ± 1°C) and humidity- (≈ 60%) controlled room. Fluorescence was monitored at right angles to the excitation path through a Karl Lambrecht MUG TS10 (angle 54°44′) polarizer, a Schott WG 345 filter and an Applied Photophysics f 4.0 monochromator by a fast photomultiplier tube (Philips XP2020Q) mounted in an Applied Photophysics voltage divider. The full width at half-maximum intensity of the scattered excitation function measured by the time-correlated fluorometer was about 300 ps. Conventional time-correlated single-photon counting detection methods were used to obtain the sample fluorescence decay and the excitation function. The start signal for the time to pulse height analyzer (TAC) was taken either from a TTL logic pulse generated from the cavity dumper and synchronized with the pulse train, or from a fast photodiode (Spectra-Physics model 403B) monitoring a fraction of the undoubled dye laser beam. Better time stability was achieved with the latter method and therefore it became the preferred way to obtain the start signal. The TAC (Ortec model 457 or Canberra model 2043) was operated in the normal configuration, the voltage ramp being initiated by the photodiode signal and terminated by a signal from the XP2020Q photomultiplier. Pulse pile-up distortion was avoided by working at an average count of 0.02–0.005 photons per excitation pulse. The output pulse of the TAC was fed into a biased amplifier (Canberra model 1467) to sample a section of the TAC range and expand it to cover the full voltage range of the multichannel analyzer (Canberra model 8100) working in pulse height

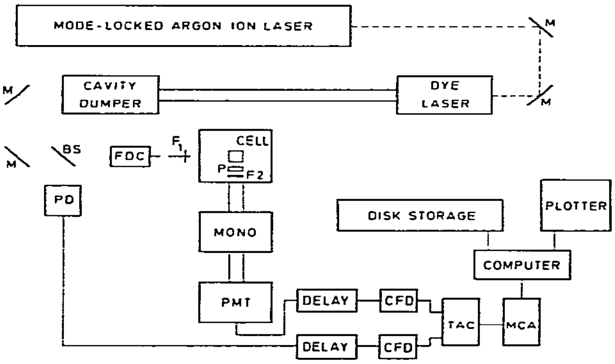

Fig. 1. Subnanosecond fluorescence spectrometer: BS, beam splitter; M, mirror; F1, Corning 7-54 filter; F2, Schott WG 345 filter; P, polarizer; PMT, XP2020Q photomultiplier tube; PD, photodiode; CFD, constant fraction discriminator; MONO, monochromator; TAC, time-to-amplitude converter; MCA, multichannel analyzer; FDC, frequency doubling crystal.

analysis mode. The bias level control was used as a zero time shift. Quad constant fraction discriminators (Ortex Model 934) were used to eliminate background pulses and to provide the correct voltage signals for the TAC. Data were collected in 256 channels of the multichannel analyzer. The monomer emission was sampled at 378 nm and the excimer emission at 490 nm. Data collection was stopped when the total number of counts of emitted photons reached about 10^6. Data accumulated in the multichannel analyzer were transferred to a Digital Equipment Corporation PDP-11/23 computer for analysis.

2.5. Theoretical decay curves used to analyze the fluorescence decay data

To analyze the data the experimental decays were fitted to several theoretical decay functions using a nonlinear least-square [17,18] decay-fitting program based on Marquardt's algorithm [19]. Four criteria were used to judge the goodness of fit [20], namely χ^2, weighted residuals (R_i), autocorrelation function (C_i) [21,22] and serial correlation coefficient [23,24]. A decay-fitting result was rejected when one of these parameters was not acceptable. The experimental fluorescence decays were analyzed using trial decay functions (eq. 1) containing one, two or three exponentially decaying terms:

$$I(t)=\sum_{i=1}^{n} A_i \exp(-\lambda_i t) \quad n=1,2,3 \tag{1}$$

where $I(t)$ is the time-dependent fluorescence intensity, A_i preexponential factors and $1/\lambda_i$ decay times. The decays of the monomer were also analyzed according to eq. 2 which takes a time dependence in the diffusion-controlled formation of excimers into account. This equation is based on the Smoluchowski diffusion theory [5].

$$I_m(t)=I_0 \exp(-At-B\sqrt{t}) \tag{2}$$

Recursion formulas derived by Liu et al. [7] were used to determine I_0, A and B. The meaning of A and B is explained further in the text.

The experimental (observed) fluorescence decay curve, $f(t)$, is a convolution of the true decay, $I(t)$, with the measured pulse shape of the excitation, $g(t)$ (the instrument response function), i.e.

$$f(t)=\int_0^t g(t')I(t-t')\mathrm{d}t' \tag{3}$$

When $f(t)$ and $g(t)$ are known $I(t)$ may be determined by a variety of techniques [17,18].

3. Results

The fluorescence kinetics of 1-methylpyrene in SUV of DMPC was studied in the temperature range 25–70 °C at four different 1-methylpyrene/DMPC molar ratios, namely, 1 : 60, 1 : 100, 1 : 200 and 1 : 2000.

Only the 1 : 2000 sample showed no steady-state excimer fluorescence spectra. All the emission spectra of the other samples showed a broad unstructured peak around 480 nm (fig. 2) due to excimer formation [2]. The fluorescence decay of the 1 : 2000 sample was monoexponential. The lifetimes of 1-methylpyrene in DMPC (ratio 1 : 2000) as a function of temperature are shown in table 1. The Arrhenius plot (ln $1/\tau_0$ as a function of $1/T$) gave a value of 4.4 kJ/mol for the activation energy of the monomolecular decay of the excited state of 1-methylpyrene in the absence of excimer formation.

For the samples that showed excimer forma-

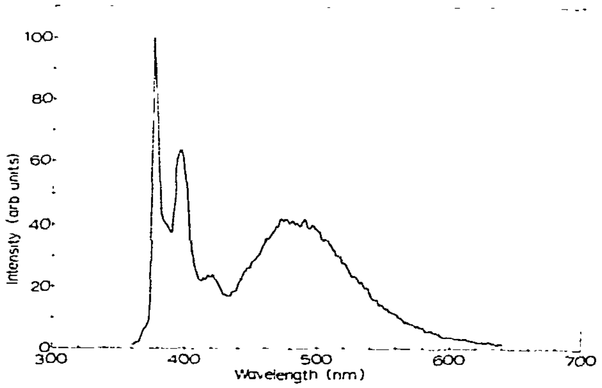

Fig. 2. Fluorescence spectrum of 1-methylpyrene in DMPC SUV. 1-Methylpyrene/DMPC ratio 1 : 60 at 55 °C. $\lambda_{exc}=343$ nm.

Table 1

Fluorescence lifetimes (τ_0) of 1-methylpyrene in DMPC SUV in the absence of excimer

λ_{exc} = 300 nm and λ_{an} = 378 nm.

T (°C)	τ (ns)
70	177.0
65	181.7
60	185.9
55	185.5
50	190.4
45	197.2
40	198.2
35	212.5
30	217.4
25	222.0
20	225.8

tion, the experimental decay of the excimer showed a rise and a decay and could be fitted to a difference of two exponential terms. An example of excimer decay is given in fig. 3.

As exemplified in fig. 4 the decay of the monomer fluorescence of 1-methylpyrene could not be fitted to a monoexponential decay function. The figure shows that there is a deviation at the beginning of the curve. The decay curves could be adequately described by two exponential terms. The decay times were close to those of the excimer region. The relative error in the short decay parameter was rather large because the contribution of the short decay time was small. When the short decay time $1/\lambda_2$ of the analysis of the excimer region was substituted in the correponding mono-

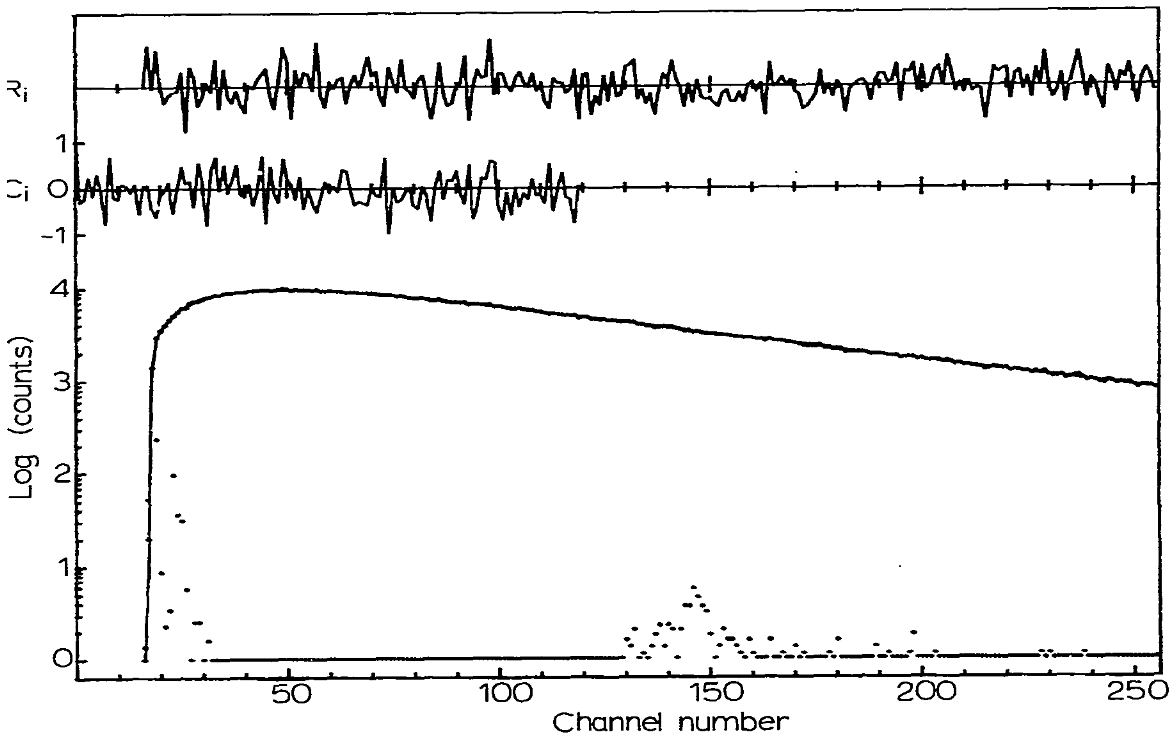

Fig. 3. Experimental fluorescence decay curve (point plot) of the excimer region of 1-methylpyrene in DMPC SUV. 1-Methylpyrene/DMPC ratio 1 : 100 at 40 °C. Analysis as a two-exponential (solid line). The instrument response function (point plot) is also shown. The decay times are shown in fig. 6. λ_{exc} = 300 nm; λ_{an} = 490 nm; channel width = 1.939 ns; R_t (max) = 4.36; χ^2 = 1.31; serial correlation coefficient D = 1.76.

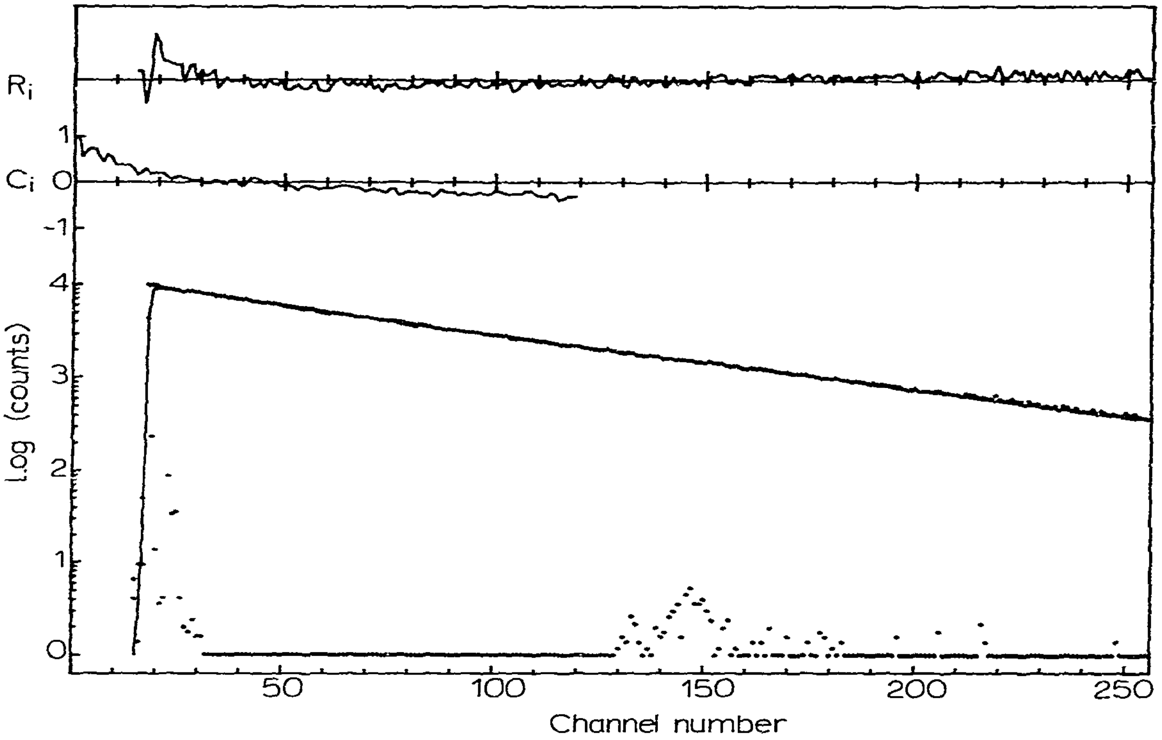

Fig. 4. Experimental fluorescence decay curve (point plot) of the monomer region of 1-methylpyrene in DMPC SUV. 1-Methylpyrene/DMPC *ratio* 1 : 100 *at* 40 °C. Analysis as a one-exponential (solid line). The instrument response function (point plot) is also shown. λ_{exc} = 300 nm; λ_{an} = 378 nm; *channel width* = 1.939 ns; R_t (max) = 12.8; χ^2 = 3.24; serial correlation coefficient D = 0.69.

Table 2

Decay parameters

1-Methylpyrene/DMPC *ratio* 1 : 60. Analysis as a two-exponential. $I_m(t) = A_1 \exp(-\lambda_1 t) + A_2 \exp(-\lambda_2 t)$ and $I_e(t) = A_3 \exp(-\lambda_1 t) + A_4 \exp(-\lambda_2 t)$.

T (°C)	Monomer region					Excimer region				
	A_2	$1/\lambda_2$ (ns)	A_1	$1/\lambda_1$ (ns)	χ^2	A_4	$1/\lambda_2$ (ns)	A_3	$1/\lambda_1$ (ns)	χ^2
70	0.30	22.5	0.70	56.1	0.96	−0.49	22.5	0.51	59.8	1.64
65	0.30	26.5	0.70	61.7	0.75	−0.49	26.5	0.51	64.3	1.01
60	0.29	29.2	0.71	65.7	0.40	−0.49	29.2	0.52	66.3	1.25
55	0.29	32.0	0.71	72.9	0.83	−0.48	32.0	0.51	72.0	0.88
50	0.25	35.5	0.75	78.8	0.74	−0.49	35.5	0.51	78.4	1.10
45	0.18	40.7	0.82	86.2	0.43	−0.49	40.7	0.51	83.2	1.76
40	0.16	41.2	0.84	100.2	0.54	−0.47	41.2	0.53	98.7	0.53
35	0.15	42.5	0.85	117.5	0.49	−0.46	42.5	0.54	115.8	0.98
30	0.12	43.4	0.88	134.6	0.34	−0.46	43.4	0.54	131.6	0.49
25	0.10	44.6	0.90	149.4	0.67	−0.45	44.6	0.55	147.6	1.29

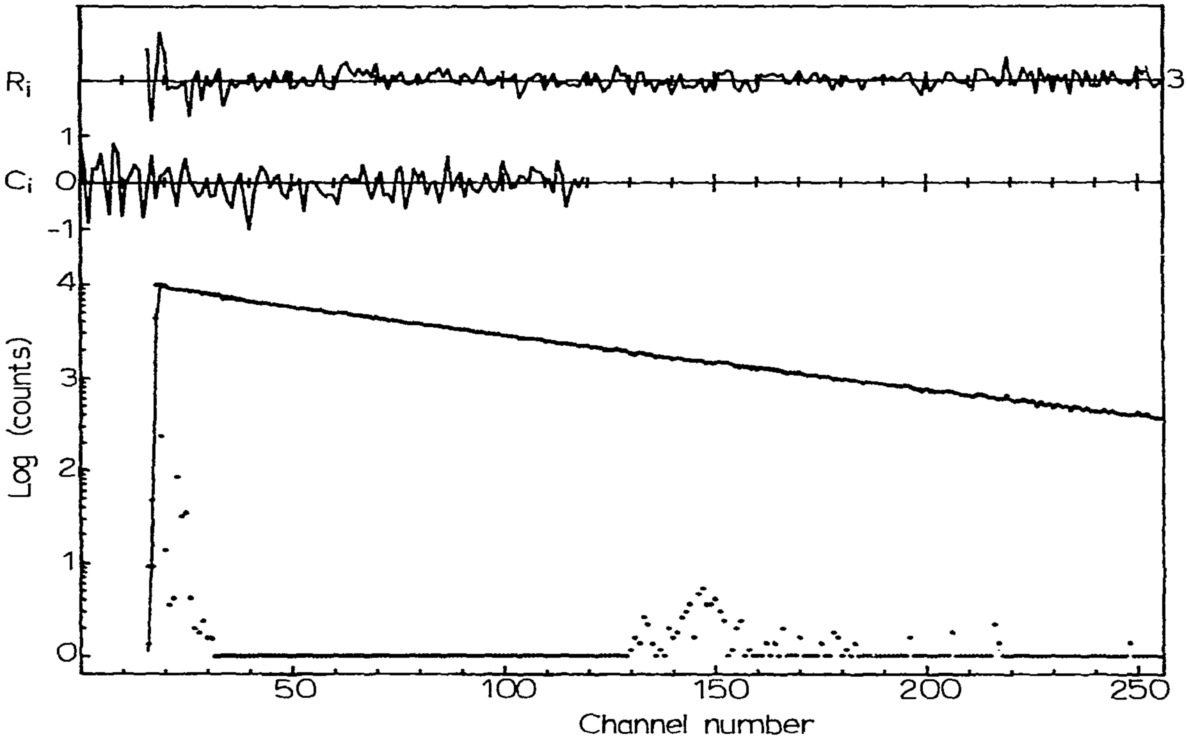

Fig. 5. Experimental fluorescence decay curve (point plot) of the monomer region of 1-methylpyrene in DMPC SUV. 1-Methylpyrene/DMPC ratio 1 : 100 at 40 °C. Analysis as a two-exponential (solid line). The instrument response function (point plot) is also shown. λ_{exc} = 300 nm; λ_{an} = 378 nm; channel width = 1.939 ns; R_r(max) = 5.42; χ^2 = 0.87; serial correlation coefficient D = 1.94.

mer decay analysis, an excellent fit was obtained. An example of a fitting result is given in fig. 5. The complete results of the decay-fitting calculations of the 1 : 60 1-methylpyrene/DMPC sample are given in table 2. The decay times and preexponential factors of all samples are given in figs. 6 and 7. Fitting the experimental decay data of the monomer fluorescence to a three-exponential trial decay function gave two identical decay times and did not result in an improvement of the fitting statistics [25].

The results in table 2 show that in the excimer region the ratio A_3/A_4 equals -0.96 ± 0.01 for the 1 : 60 1-methylpyrene/DMPC sample above 45 °C and -0.85 ± 0.02 in the temperature region 25–40 °C. For the 1 : 100 1-methylpyrene/DMPC sample the A_3/A_4 ratio equals -0.84 ± 0.05 over the whole measured temperature range (25–70 °C) and for the 1 : 200 1-methylpyrene/DMPC sample A_3/A_4 equals -0.74 ± 0.1 between 40 and 70 °C. For the 1 : 200 sample below 40 °C excitation light scatter became too dominant so that reliable data analysis became virtually impossible.

The decay times $1/\lambda_1$ and $1/\lambda_2$ decrease with rising temperature in the three samples (1 : 60, 1 : 100 and 1 : 200) in both monomer and excimer regions. In the monomer region the contribution of the short decay time $1/\lambda_2$ is small compared with that of the long decay parameter $1/\lambda_1$. The agreement between the mean decay parameters $1/\lambda_1$ in the monomer and excimer regions is excellent. The relative contribution of the short decay time $1/\lambda_2$ rises with increasing temperature. With increasing probe/phospholipid ratio, there is a

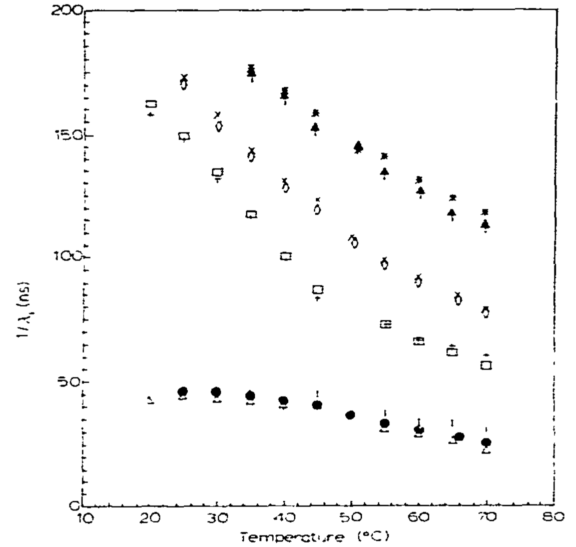

Fig. 6. Experimentally determined decay times of the monomer region of 1-methylpyrene in DMPC SUV in different ratios (1 : 60, 1 : 100, 1 : 200) and at different temperatures. Analysis as a two-exponential. $I_m(t) = A_1 \exp(-\lambda_{1M}t) + A_2 \exp(-\lambda_{2M}t)$ for the monomer region and $I_e(t) = A_3(\exp - \lambda_{1E}t) + A_4 \exp(-\lambda_{2E}t)$ for the excimer region. (△) $1/\lambda_{2M}$, $1/\lambda_{2E}$ (1 : 60), (□) $1/\lambda_{1M}$ (1 : 60), (+) $1/\lambda_{1E}$ (1 : 60), (●) $1/\lambda_{2M}$, $1/\lambda_{2E}$ (1 : 100), (×) $1/\lambda_{1M}$ (1 : 100), (◇) $1/\lambda_{1E}$ (1 : 100), (|) $1/\lambda_{2M}$, $1/\lambda_{2E}$ (1 : 200), (*) $1/\lambda_{1M}$ (1 : 200), (↑) $1/\lambda_{1E}$ (1 : 200)

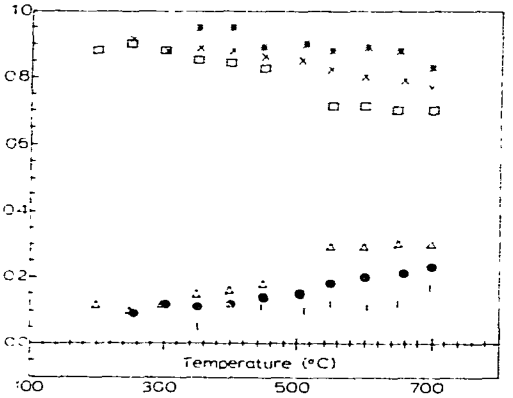

Fig. 7. Experimentally determined preexponential factors of the monomer region of 1-methylpyrene in DMPC SUV in different ratios (1 : 60, 1 : 100, 1 : 200) and at different temperatures. (△) A_2 (1 : 60), (□) A_1 (1 : 60), (●) A_2 (1 : 100), (×) A_1 (1 : 100), (|) A_2 (1 : 200), (*) A_1 (1 : 200).

strong decrease in $1/\lambda_1$ in both monomer and excimer regions. The contribution of the short decay time ($1/\lambda_2$) increases with increasing probe concentration. The excited-state processes in the excimer formation are depicted in scheme I [2,3,26], where k_3 is the rate constant of excimer formation, k_4 is the rate constant of excimer dissociation, k_1 and k_5 are the rate constants of fluorescence of the monomer and excimer respectively and k_2 and k_6 are the rate constants of the non-radiative decay of the monomer and excimer respectively.

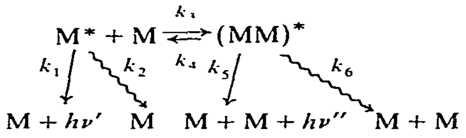

Scheme I.

Following this scheme the fluorescence decays of the monomer $I_m(t)$ and excimer $I_e(t)$ are given by eqs. 4 and 6.

$$I_m(t) = A_1 \exp(-\lambda_1 t) + A_2 \exp(-\lambda_2 t) \tag{4}$$

$$A_1/A_2 = (X - \lambda_2)/(\lambda_1 - X) \tag{5}$$

$$I_e(t) = A_3 \exp(-\lambda_1 t) + A_4 \exp(-\lambda_2 t)$$
$$\text{and } A_3 = -A_4 \tag{6}$$

$$\lambda_{1,2} = 0.5\left\{(X + Y) \mp \left[(X - Y)^2 + 4k_3k_4[\mathrm{M}]\right]^{1/2}\right\} \tag{7}$$

$$X = k_1 + k_2 + k_3[\mathrm{M}] \tag{8}$$

$$Y = k_5 + k_6 + k_4 \tag{9}$$

$$\tau_e = 1/Y \tag{10}$$

Applying scheme I to our experimental data (tables 1 and 2, figs. 6 and 7), the apparent rate constants of excimer formation (k_3[M]) and the excimer lifetimes (τ_e) could be determined as a function of temperature and probe concentration. The results of these calculations are presented in table 3. To give an estimation of the rate constant k_3 of the excimer formation and of the associated diffusion constant, D, the probe concentration [M] must be known. This implies knowledge of the volume in which the probe can move and this was estimated as follows: A value of 2 nm [30] was

Table 3

k_3[M], k_3, D and $1/Y$ (excimer lifetime) as a function of temperature and 1-methylpyrene/DMPC ratios

T (°C)	1-Methylpyrene/DMPC											
	1:60				1:100				1:200			
	k_3[M] (s^{-1}) ($\times 10^{-6}$)	k_3 ($l\ mol^{-1}\ s^{-1}$) ($\times 10^{-8}$)	D_{diff} (m^2/s) ($\times 10^{10}$)	$1/Y$ (ns)	k_3[M] (s^{-1}) ($\times 10^{-6}$)	k_3 ($l\ mol^{-1}\ s^{-1}$) ($\times 10^{-8}$)	D_{diff} (m^2/s) ($\times 10^{10}$)	$1/Y$ (ns)	k_3[M] (s^{-1}) ($\times 10^{-6}$)	k_3 ($l\ mol^{-1}\ s^{-1}$) ($\times 10^{-8}$)	D_{diff} (m^2/s) ($\times 10^{10}$)	$1/Y$ (ns)
70	20.8	7.5	2.0	27.4	13.6	8.0	2.1	29.9	6.8	8.1	2.1	35.6
65	17.2	6.2	1.6	31.9	11.5	6.9	1.8	32.1	5.2	6.2	1.6	36.9
60	15.2	5.5	1.4	34.8	9.7	5.8	1.5	35.8	4.6	5.5	1.4	37.4
55	13.2	4.7	1.2	37.8	8.3	5.0	1.3	38.2	4.0	4.8	1.3	41.3
50	11.3	4.0	1.1	41.7	6.7	4.0	1.0	41.1	3.7	4.4	1.2	48.9
45	8.4	3.0	0.79	45.0	5.4	3.2	0.83	44.6	3.0	3.6	0.94	46.0
40	7.2	2.6	0.67	45.5	4.5	2.6	0.69	46.3	2.0	2.4	0.63	–
35	7.0	2.5	0.65	47.0	3.9	2.3	0.60	48.3	–	–	–	–
30	4.7	1.7	0.44	47.2	3.6	2.1	0.55	50.2	–	–	–	–
25	3.8	1.4	0.36	48.0	2.7	1.6	0.42	49.5	–	–	–	–

taken for Z, the thickness of the membrane in which the probe can diffuse. The radius of SUV is 12.5 ± 2.5 nm [11]. Using these values and assuming a value of 2800 [11] for the aggregation number of SUV, the probe concentration [M] and hence the rate constant k_3 could be calculated for different probe/lipid ratios. For the diffusion of 1-methylpyrene in a two-dimensional system the diffusion coefficient, D, is given by eq. 11 [30].

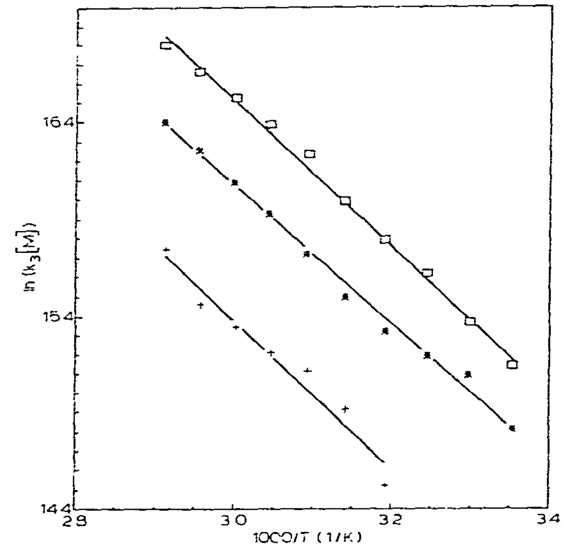

Fig. 8. Determination of the activation energy of the apparent excimer formation rate constant k_3 [M] in different 1-methylpyrene/DMPC ratio (1 : 60, 1 : 100, 1 : 200). (□) 1 : 60, (∗) 1 : 100, (+) 1 : 200.

$$D = k_3/(3.17ZN') \qquad (11)$$

where N' is Avogadro's number per mmol and Z the thickness of the two-dimensional system. The estimated k_3 and D values are given in table 3. The activation energy for the diffusion-controlled excimer formation process was calculated and found to be 31.6, 30.0 and 28.2 kJ/mol for the 1 : 60, 1 : 100 and 1 : 200 1-methylpyrene/DMPC samples respectively. This is shown in fig. 8 which gives an average value of 29.9 ± 1.4 kJ/mol for the activation energy of the diffusion of 1-methylpyrene in SUV of DMPC.

Eq. 2 could also be used to analyze the monomer decays of 1-methylpyrene that was incorporated into DMPC SUV. This decay function takes a time dependence in the diffusion-controlled formation process of excimers into account [5]. Good fits to this equation were obtained for the whole temperature region and for all probe/lipid ratios. The decay fitting results are given in table 4 and an example is shown in fig. 9. The processes considered in the excimer formation are given in scheme II [2,3,27]. Excimer dissociation is neglected in this model.

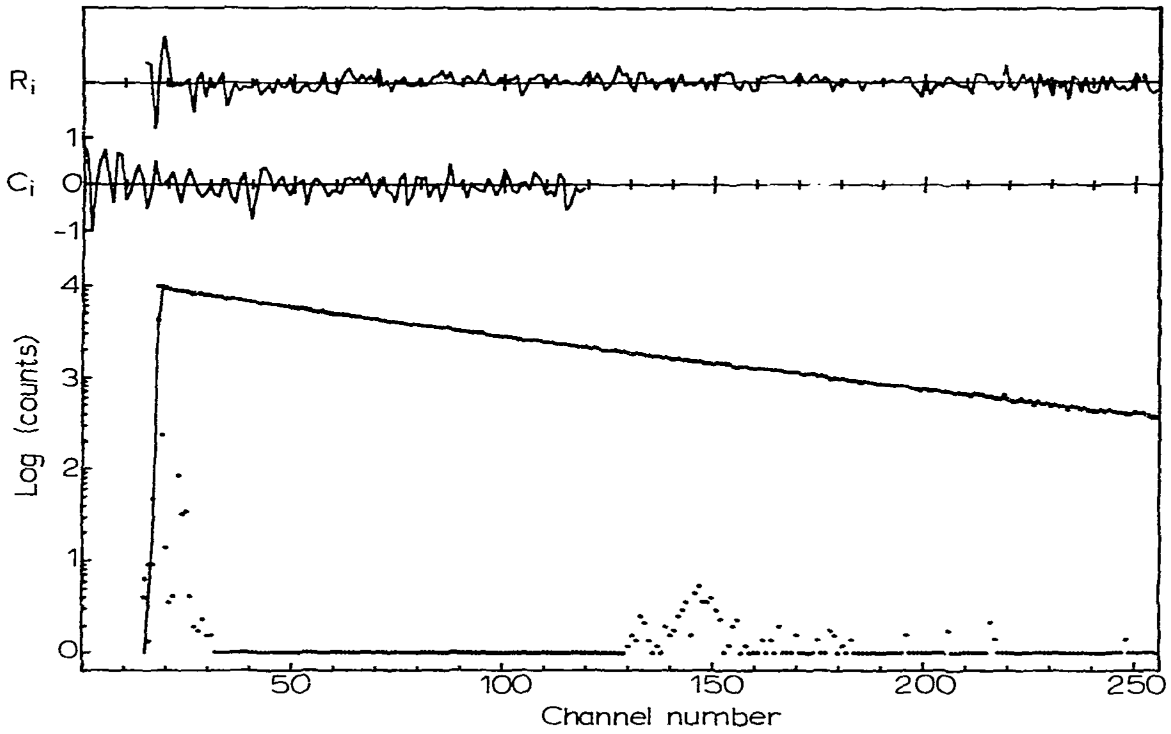

Fig. 9. Experimental fluorescence decay curve (point plot) of the monomer region of 1-methylpyrene in DMPC SUV. 1-Methylpyrene/DMPC ratio 1 : 100 at 40 °C. Analysis according to eq. 2 (solid line). The instrument response function (point plot) is also shown. $\lambda_{exc} = 300$ nm; $\lambda_{an} = 378$ nm; channel width = 1.939 ns; R_t (max) = 5.52; $\chi^2 = 0.82$; serial correlation coefficient $D = 2.04$.

Table 4

Decay curve-fitting results of 1-methylpyrene in DMPC vesicles at different probe/lipid ratios as a function of temperature (eq. 2)

T (°C)	1-Methylpyrene/DMPC					
	1 : 60		1 : 100		1 : 200	
	$1/A$ (ns)	B ($s^{-1/2}$)	$1/A$ (ns)	B ($s^{-1/2}$)	$1/A$ (ns)	B ($s^{-1/2}$)
70	66.7	2403	83.6	980	127.3	506
65	–	–	92.9	1170	133.3	560
60	–	–	101.1	1043	139.8	443
55	80.8	1612	107.3	917	149.3	427
50	–	–	114.9	695	151.9	379
45	98.8	822	131.6	632	165.4	313
40	106.0	727	139.4	537	172.2	147
35	122.1	739	150.6	433	–	–
30	–	–	165.6	376	–	–
25	157.4	398	179.6	265	–	–

$$\begin{array}{ll}
\text{Process} & \text{Rate} \\
\mathrm{M} \xrightarrow{h\nu} \mathrm{M}^* & \\
\left.\begin{array}{l} \mathrm{M}^* \longrightarrow \mathrm{M} + h\nu' \\ \mathrm{M}^* \longrightarrow \mathrm{M} \end{array}\right\} & 1/\tau_0\,[\mathrm{M}^*] \\
\mathrm{M}^* + \mathrm{M} \longrightarrow (\mathrm{MM})^* & k_3(t)[\mathrm{M}][\mathrm{M}^*]
\end{array}$$

Scheme II

M denotes the monomer, M* the excited state of the monomer, (MM)* the excimer, $1/\tau_0$ the fluorescence lifetime of M* in the absence of complex formation and $k_3(t)$ is a time-dependent rate constant [27,28]. For a three-dimensional system eq. 2 is explicitly given by eq. 12.

$$I(t) = I_0 \exp\left\{-\left[1/\tau_0 + 4\pi N'R'D'\left(1 + 2R'/\sqrt{\pi D't}\right)[M]\right]t\right\} \tag{12}$$

where R' is twice the interaction radius of monomeric 1-methylpyrene, D' twice the diffusion coefficient of 1-methylpyrene, and [M] the monomer concentration. For the diffusion of 1-methylpyrene in a two-dimensional system the parameters A and B are given by eq. 13 and 14 [29].

$$A = 1/\tau_0 + 1.585ZD'N'[M] \tag{13}$$

$$B = 7.09ZN'R'[M]D'^{1/2} \tag{14}$$

where Z is the thickness of the two-dimensional system.

Table 5

Calculated D values using eq. 15 for different temperatures and 1-methylpyrene/DMPC ratios

T (°C)	D (m²/s) (×10¹⁰)		
	1:60	1:100	1:200
70	0.65	1.80	0.80
65	–	0.90	0.55
60	–	0.80	0.70
55	0.80	0.80	0.40
50	–	1.05	0.50
45	1.65	0.70	0.40
40	1.60	0.70	0.80
35	0.90	0.85	–
30	–	0.65	–
25	0.95	0.70	–

Eq. 15 can be derived from eq. 13 and 14.

$$D' = \left[(A - 1/\tau_0)4.47R'/B\right]^2 \tag{15}$$

Values for the diffusion constant, D, calculated according to eq. 15 with $R' = 6.6A$ [30] are of the order of 10^{-10} m²/s (table 5).

4. Discussion

The results show clearly that the fluorescence decay of monomeric 1-methylpyrene in SUV of DMPC above the phase transition can be fitted to a two-exponentional decay function and to a decay law which takes the time dependence of the rate constant of excimer formation into account. The excimer decay can be adequately described by a two-exponential decay function. When applying scheme I, the ratio between the preexponentional factors A_3/A_4 in the excimer region must be equal to negative unity. When the ratio of excimer fluorescence to excitation light scattering is high the ratio A_3/A_4 approaches the theoretical value of -1 (1-methylpyrene/DMPC sample 1 : 60 between 45 and 70 °C). When the contribution of the excitation light scattering becomes larger, the early part of the experimenal decay is influenced which results in deviation of A_3/A_4 from -1. This is the case when the 1-methylpyrene/DMPC ratio decreases (1 : 100 and 1 : 200 1-methylpyrene/DMPC samples) or when the temperature is lowered beneath the phase transition temperature. For the monomer region the fluorescence/excitation light scatter ratio was always large enough, so that the influence of light scatter on the decay curves was minimal.

The physical meaning of the different decay times in the excimer region becomes clear when the decay of the locally excited state of the probe is analyzed at the same temperature. In the monomer region the same decay times were found as in the excimer region which is a good indication that the well-known scheme for excimer formation in a homogeneous solution can be applied. The results in table 2 show that $1/(k_3[\mathrm{M}] + k_2 + k_1)$ is approximated by $1/\lambda_1$ and $1/Y$ is approximated by $1/\lambda_2$. The measured decay of the excimer is not the lifetime of the excimer $1/Y$. This is due to the fact that the sum of the rate constants of the monomer (X) is much smaller than the sum of the rate constants of the excimer (Y). X is low because the concentration of 1/methylpyrene in the bilayer is kept low. To check the above, the fluorescence decay of 1-methylpyrene in isooctane was measured at low concentration (1.2×10^{-4} M) in the temperature region −70 to 0°C. The fluorescence decay was monoexponential. The monomer decay time ($1/\lambda_1$) varied from 236 ns at −70°C to 160 ns at 0°C. In the excimer region the decay showed a rise ($1/\lambda_2$) and a decay which was equal to $1/\lambda_1$ of the monomer region at all temperatures. For the rise in the excimer region a lifetime of 60 ns was measured independently of the temperature. From these data it was concluded that A_2 was very small, i.e., $A_2 \cong 0$, and using eq. 5 it can easily be seen that $\lambda_1 \cong X$. λ_2 can be calculated from eq. 7, i.e., $\lambda_2 \cong Y$. The lifetime of the excimer is not given by the decay of the excimer fluorescence but by the rise of the excimer fluorescence signal. It is necessary to measure the monomer decay to interpret the data of the excimer region. Pyrene has been used by Galla et al. [31–33] to determine diffusion coefficients of this probe in vesicle systems using the fluorescence intensities of monomer (I_m) and excimer (I_e) and the 'single excimer lifetime' τ_0' (eq. 16).

$$D = K\frac{I_e}{I_m \tau_0' [M]} \tag{16}$$

where K is a proportionality constant [1] and [M] the probe concentration. τ_0' was determined by laser flash spectroscopy [32]. Their measured single excimer lifetimes were strongly temperature dependent (170 ns at 25°C and 65 ns at 65°C). Using the time-correlated single-photon counting technique, we measured excimer lifetimes varying from 50 ns at 25°C to 30 ns at 70°C. However, the decay times of the excimer ($1/\lambda_1$) are much longer. The decay time ($1/\lambda_1$) in the excimer region is only a parameter and not a priori the excimer lifetime. This has possibly been overlooked by these authors.

The results in table 3 show that the calculated excimer lifetimes are approximately independent of the probe concentration which is predicted by the model presented in scheme I.

The activation energy for the diffusion-controlled excimer formation of 1-methylpyrene in SUV of DMPC above the phase transition is somewhat lower than the value determined by Galla and Sachmann [31] for the diffusion of pyrene in sonicated vesicles above the phase transition temperature using stationary methods and the single excimer lifetime.

The monomer decays could also be analyzed according to eq. 2. Diffusion coefficients of 1-methylpyrene were calculated (eq. 15) assuming diffusion in a two-dimensional system [6,29]. Although diffusion theories describing the variation of the diffusion coefficient as a function of temperature and viscosity are rather complex, eq. 17 approximates the relation [34]:

$$\frac{\eta D}{T} = \text{constant} \tag{17}$$

where D is the diffusion coefficient, η the viscosity of the solvent and T the absolute temperature. Eq. 17 predicts an increase for D with increasing temperature. The experimentally determined D values (table 5) do not increase significantly with increasing temperature. The relative variation of the B value (eq. 14) as a function of temperature must be less than the relative variation of A (eq. 13) as a function of temperature because in the two-dimensional model, as well as in the three-dimensional model (eq. 12), A is related to D and B is related to $D^{1/2}$. Experimentally this is not found. It can therefore be concluded that the observed decays are not compatible with a reaction scheme which takes a time dependence of the rate constant of excimer formation into account.

The D values listed in table 3 are independent of the probe concentration and increase with increasing temperature according to eq. 17. The D values vary between 4×10^{-11} m^2/s at 25°C and 2×10^{-10} m^2/s at 70°C. These values indicate that the fluidity of the membrane is rather low compared with the fluidity of most isotropic solvents. The D values for 1-methylpyrene in SUV of DMPC determined in the present work are somewhat higher than those found in the literature: pyrene in dipalmitoylphosphatidylcholine

(DPPC) multilamellar vesicles (1×10^{-11} m^2/s at 45 °C) [1]; pyrene in DMPC sonicated vesicles (3×10^{-12} m^2/s at 30 °C) [4]; pyrene/*N,N*-dimethylaniline in DPPC sonicated vesicles (4.7×10^{-11} at 50 °C) [30] and 10-pyrenyldecanoic acid/*N,N*-dimethylaniline in DPPC sonicated vesicles (3.1×10^{-11} m^2/s at 50 °C) [30].

Our results show that the kinetic scheme of excimer formation in a homogeneous medium can be used to describe the excimer formation of 1-methylpyrene in SUV of DMPC above the phase transition temperature. It has been shown that one has to be very careful in interepreting the data of the excimer region in order to elucidate the significance of the different calculated parameters, especially when the probe/lipid ratio is low. The activation energy of the formation of excimer was found to be 29.9 ± 1.4 kJ/mol. The excimer lifetimes could be determined and are of the order of 30–50 ns in the temperature domain (25–70 °C) studied and are independent of the probe/lipid ratio.

Acknowledgments

This investigation was supported by grants from the F.K.F.O. and the University Research Fund. M.V.d.Z. is a predoctoral fellow of the I.W.O.N.L. (Belgium). N.B. is a Research Associate of the National Fund for Scientific Research (Belgium).

References

1 H.-J. Galla and E. Sackmann, Biochim. Biophys. Acta 339 (1974) 103.
2 J.B. Birks, D.J. Dyson and I.H. Munro, Proc. R. Soc. A275 (1963) 575.
3 J.B. Birks, M.D. Lumb and I.H. Munro, Proc. R. Soc. A280 (1964) 289.
4 J.M. Vanderkooi and J.B. Callis, Biochemistry 13 (1974) 4000.
5 M. Smoluchowski, Z. Phys. Chem. 92 (1917) 129.
6 J.M. Vanderkooi, S. Fischkoff, M. Andrich, F. Podo and C.S. Owen, J. Chem. Phys. 63 (1975) 3661.
7 B.M. Liu, H.C. Cheung, K.-H. Chen and M.S. Habercom, Biophys. Chem. 12 (1980), 341.
8 Y. Barenholz, D. Gibbes, B.J. Litman, J. Goll, T.E. Thompson and F.D. Carlson, Biochemistry 16 (1977) 2806.
9 B.P. Gaber and J.P. Sheridan, Biochim. Biophys. Acta 685 (1982) 87.
10 Huang-Minlon, J. Am. Chem. Soc. 68 (1946) 2487.
11 C. Huang, Biochemistry 8 (1969) 344.
12 J. Suurkuusk, B.R. Lentz, Y. Barenholz, R.L. Biltonen and T.E. Thompson, Biochemistry 15 (1976) 1393.
13 M. Wong and T.E. Thompson, Biochemistry 21 (1982) 4133.
14 M. Petitou, F. Tuy and C. Rosenfeld, Anal. Biochem. 91 (1978) 350.
15 K.G. Spears, L.E. Cramer and L.D. Hoffland Rev. Sci. Instrum. 49 (1978) 255.
16 B.T. Turko, J.A. Nairn and K. Sauer, Rev. Sci. Instrum. 54 (1983) 118.
17 A.E. McKinnon, A.G. Szabo and D.R. Miller, J. Phys. Chem. 81 (1977) 1564.
18 D.V. O'Connor, W.R. Ware and J.C. Andre, J. Phys. Chem. 83 (1979) 1333.
19 D.W. Marquardt, J. Soc. Indust. Appl. Math. 11 (1963) 431.
20 A.J. Roberts, D. Phillips, F.A.M. Abdul-Rasoul and A. Ledwith, J. Chem. Soc. Faraday Trans. 1, 77 (1981) 2725.
21 J.H. Easter, R.P. DeToma and L. Brand, Biophys. J. 16 (1976) 571.
22 A. Grinvald and I.Z. Steinberg, Anal. Biochem. 59 (1974) 583.
23 J. Durbin and G.S. Watson, Biometrika 37 (1950) 409.
24 J. Durbin and G.S. Watson, Biometrika 38 (1951) 159.
25 M. Ameloot and H. Hendrickx, J. Chem. Phys. 76 (1982) 4419.
26 T. Förster and K. Kasper, Z. Phys. Chem. N.F. 1 (1954) 275.
27 J. Yguerabide, M.A. Dillon and M. Burton, J. Chem. Phys. 40 (1964) 3040.
28 R.W. Ware and J.S. Novros, J. Phys. Chem. 70 (1966) 3246.
29 C.S. Owen, J. Chem. Phys. 62 (1975) 3204.
30 K. Kano, H. Kawazumi, T. Ogawa and J. Sunamoto, J. Phys. Chem. 85 (1981) 2204.
31 H.-J. Galla and E. Sachmann, Ber. Bunsenges. Phys. 78 (1974) 949.
32 H.-J. Galla, W. Hartmann, U. Theilen and E. Sachmann, J. Membrane Biol. 48 (1979) 215.
33 H.-J. Galla and W. Hartmann, Chem. Phys. Lipids 27 (1980) 199.
34 J.B. Birks, in: Photophysics of aromatic molecules (Wiley-Interscience, New York, 1970) p. 312.